



Research Article

## Numerical investigation of the heat transfer enhancement inside a square duct with rectangular vortex generators

Mustafa J. AL-DULAIMI<sup>1\*</sup>, Fadhil Abdulrazzaq KAREEM<sup>2</sup>, F. A. HAMAD<sup>3</sup>

<sup>1</sup>Department of Air Conditioning & Refrigeration Technologies Engineering,  
Al-Esraa University College, Baghdad, Iraq

<sup>2</sup>Institute of Technology Baghdad, Middle Technical University, Baghdad, Iraq

<sup>3</sup>School of computing, Engineering and Digital technology, Teesside University, UK

### ARTICLE INFO

#### Article history

Received: 19 July 2020

Accepted: 20 November 2020

#### Keywords:

Heat Transfer, Pressure Drop,  
Rectangular Vortex Generators,  
Heat Exchanger, Square Duct

### ABSTRACT

This paper investigates numerically the influence of detached square vortex generator (VGs) on the heat transfer and pressure drop inside a square duct. Reynolds number is fixed at 5000. The geometrical parameters in this investigation are: i) The blocking ratios are 0.1, 0.15 and 0.2), ii) Vortex generator numbers are 1, 2, and 3), iii) Attack angles are 0, 30, and 45, iv) The aspect ratios are 1, 1.5 and 2. The numerical simulation is carried out using ANSYS FLUENT 15. The results show that the rectangular vortex generators have a positive influence on heat transfer as a result of the augmentation in turbulence level. The maximum enhancement in average heat transfer could reach 40%. The heat transfer is found to increase with the blocking ratio. The heat transfer enhanced by 17% for one VG and 28% for 3 VGs for blocking ratio = 0.2. The VGs at angle value of 45° produce the highest heat transfer enhancement. The aspect ratio is found to have an adverse effect on heat transfer rate.

**Cite this article as:** Mustafa J. A, Fadhil A K, Hamad F A. Numerical investigation of the heat transfer enhancement inside a square duct with rectangular vortex generators. J Ther Eng 2022;8(1):1–13.

### INTRODUCTION

Heat transfer enhancement is any process objectives to improve the performance of a heat system or to increase heat transfer coefficient through utilization of various techniques. Heat transfer enhancement grows significantly in recent years as it contributes in reducing the use of the fossil fuel which lead to a reduction in emissions of carbon-dioxide and the effect of greenhouse reduced. Furthermore, save

fuel as the worldwide increase in energy demand as population increased [1]. Heat transfer enhancement techniques segregated in two major categories: passive and active techniques. In active techniques external power contribution during operation is required to improve heat transfer such as electric or acoustic fields, surface fluid vibration etc.. In passive techniques, no additional power input

#### \*Corresponding author.

\*E-mail address: [mustafa@esraa.edu.iq](mailto:mustafa@esraa.edu.iq)

This paper was recommended for publication in revised form by Regional Editor Jovana Radulovic



during operation is required but special surface geometries were fitted throughout the various industrial processes. The additional power needed to enhance heat transfer is taken from the power in a system, which eventually leads to increase in pressure drop. It is essentially employed by inserting simple geometry in the flow passage or adding fluid additives. These surfaces perform good fluid mixing and increase both turbulence and heat transfer area [2]. Passive techniques can be achieved by providing various roughen surfaces or tabulators in addition to adding vortex generators, which create three-dimensional fluid mixing through generating transverse or longitudinal vortices in the flow field [3].

Mundhe and Bindu [4] investigated experimentally and numerically the enhancement of convection heat transfer inside a heated pipe by using conical vortex generators. Fluent software was implemented to investigate the effect of ratio of pitch to diameter and the angle of attack for Reynolds number in range of 4000-5000. The results showed that Nusselt number increases with the decrease of the ratio of pitch to diameter. Maximum heat transfer enhancement was found when the angle of attack is 60°. Zeeshan et al [5] conducted a numerical study to examine the effect of introducing rectangular vortex generators incorporated with circular, flat and oval tubes on the heat transfer inside a heated channel. Three configurations, rectangular VGs behind circular tubes, rectangular VGs behind flat tubes and rectangular VGs behind oval tubes, were tested to reach the optimum configuration. The results showed that there was a significant enhancement in thermal performance. The shape of the tube had a significant influence on the heat transfer. The optimum configuration was rectangular VGs with oval tubes which increase the heat transfer by 13.8% and 10% for  $Re = 400$  and  $900$ . Sheikzadeh et al [6] investigated numerically the effect of introducing different wing shape vortex generators on the heat transfer of nanofluid inside a heated channel. Three different shape of VGs are implemented including trapezoidal, rectangular and triangular. The VGs were fixed in rows of three elements, one row was fixed on the top plate and one on the bottom plate of the channel. The working fluid consisted of ethylene glycol as a base fluid and MgO-MWCNT as suspended nanoparticles with volume fraction of 0.1%, 0.2% and 0.4%. For Reynolds number in range of 200–1600, the results showed that the rectangular VGs led to the highest heat transfer enhancement and this enhancement increases with the nanofluid volume fraction.

DongxuJin [7] investigated numerically the influence of v-shaped VGs fixed on the absorber plate on the thermal and hydraulic performance of solar air heater. Three-dimensional simulation was conducted with FluentSOFTWARE by implementing the turbulence model RNG k- $\epsilon$ . The effect of VGs on the Nusselt number and friction factor was investigated. The results showed that v-shaped VGs generate helical vortex which lead to better

mixing of the fluid which in turn enhances heat transfer. The thermal performance was almost doubled (1.93) compared to the performance without VGs. Han and et al [8] conducted a numerical simulation to investigate the heat transfer enhancement and flow characteristics in a heated duct in the presence of rectangular VGs with and without holes. The range of  $Re$  was between 214 and 10703. The effects of the diameter and the position of the holes were investigated. The results showed that the performance factor is larger for the VGs with holes. Zhang and Wang [9] performed a numerical simulation to investigate the influence of rectangular winglet pair fixed on the bottom of air heated duct on the rate of heat transfer. The range of Reynolds number was between 500 and 7000. The effects of attack angle and the height of VGs were investigated. The results showed that the presence of VGs on the bottom of the duct significantly enhances the heat transfer. It was concluded that the maximum heat transfer rate occurs when the angle of attack is 29°. Xie et al [10] investigated numerically the augmentation of heat transfer in a heated channel downstream the square VGs. Reynolds number ranged between 20,000 and 160,000 based on the inlet hydraulic diameter. Six configurations of VGs were tested. All cases indicated that the VGs presence improves heat transfer rate due to the vortices generation and better mixing. Zheng et al [11] performed a numerical simulation to study the thermal heat transfer performance in a heat exchanger tube with double inclined VGs. Preliminary numerical simulations were conducted using turbulence models including the realizable k- $\epsilon$  model, the standard k- $\omega$  model and the SST k- $\omega$  model to investigate the effect of the turbulence model. The results from all the models were in good agreement with experimental results. The results demonstrated that thermal heat transfer and friction factor in the ribbed tube was more than smooth tube by approximately 1.8 - 3.6 times and 2.1–5.6 times respectively. It can be clearly observed that vortex or swirl flow pattern generated in the tube with VGs due to turbulent mixing between the flow regions, improve the thermal heat transfer performance. Pourfattah et al [12] performed a numerical simulation to investigate the characteristics of heat transfer and flow of a nanoparticles fluid flow in a tube in the presence of a rectangular VGs. The aim was to investigate the effect of VGs attack angle in Reynolds number range of (24,000-60,000). The numerical results showed a good coincidence with those from empirical equations. The results demonstrated that the heat transfer is augmented due to the better mixing caused by eddies created by the VGs. The maximum thermal performance coefficient obtained when the attack angle is 60°. Yadov and Bhagoria [13] investigated numerically the effect of the fixing square VGs inside a duct on the heat transfer. Fluent software version 15 is used to simulate the fully developed turbulent flow using RNG k- $\epsilon$  model. The Reynolds number was between 3800 and 18,000. The effect of twelve configurations of different pitch and height

of the VGs were investigated. All the cases showed significant enhancement in heat transfer. The maximum enhancement in Nusselt number was found to be 2.86 times that of smooth duct.

Based on the study of literature, it can be concluded that vortex generators help to improve the thermal performance of thermal systems but at the expense of pressure drop. The objectives of this work is to investigate numerically the effect of rectangular VGs fixed on the middle distance between the bottom and the top of a heated duct using the commercial code Fluent software . The effects of blocking ratio (BR: height of the VG to the duct height), VGs number, attack angle ( $\theta$ ) and the aspect ratio (AR) on the heat transfer and the pressure drop inside a square duct is investigated numerically.

### NUMERICAL SIMULATION

CFD (Computational Fluid Dynamics) is analyzing systems which including fluid flow, heat transfer and any linked phenomena for example chemical reaction via computer-based simulation. Construction for the mathematical model is accomplished by grouping of mathematical equations which describe the flow. Then these equations are solved by means of a computer program with the aim of getting flow variables all over the flow field. The CFD analysis have a number of stages including the creation the domain, mesh generation, setting

boundary conditions, calculation of solution and post processing. The governing equations are presented as well as approach that has been used to solve the governing equations.

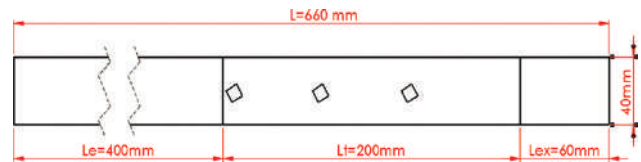


Figure 1. Side view of 3-D computational domain.

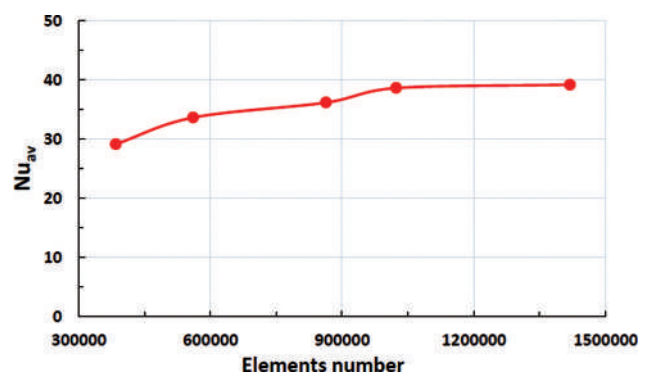


Figure 2. Variation of average Nusselt number with elements number.

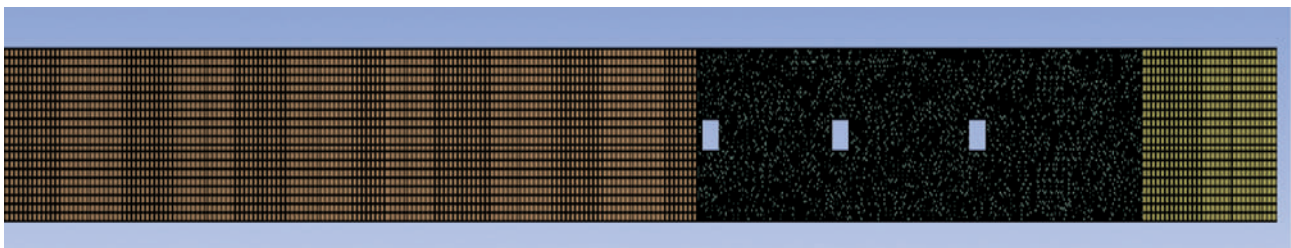


Figure 3. Side view of the meshed model.

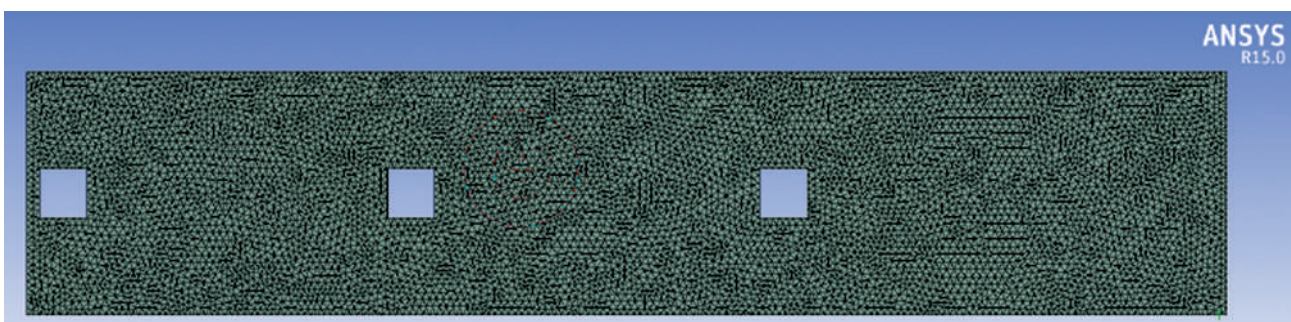


Figure 4. Side view of the meshed test region.

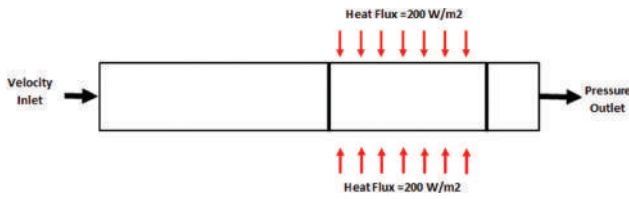


Figure 5. The boundary conditions.

### Model Creation

The geometry of flow domain has been created using SolidWork. The computational domain is represented by three regions of square section of  $4 \times 4 \text{ cm}^2$ . The first region is the entrance region; its length is 40 cm ( $10D_h$ ) to ensure fully developed flow [14]. The second region is the test section, its length is 20 cm. The VGs are fixed in the test section at the centre line. The third region is the exhaust region which connects the test region with ambient, It is of 6 cm in length. This region separates the test region from the effects of the ambient. Figure 1 shows the side view of the 3D model.

### Grid Creation

The flow region is divided into extremely small components, and the governing equations for these small elements are solved, resulting in the generation of a computational grid or mesh. Structured and unstructured meshing are the two types of volume meshing procedures employed [15]. Because the entrance and exit areas have the same section, structured hexagonal meshing is employed to mesh them. Because the test region is non-uniform due to the existence of VGs, unstructured Tetrahedron meshing is applied. The size of the elements has a substantial impact on the simulation results; however, in this study, the element size is only relevant in the test region because it involves fluid flow and heat transfer. Figure 2 depicts the effect of element number on average Nusselt number in the test section. When the average Nusselt number becomes practically constant with the change in grid size, 1420557 was chosen as the grid size. The boundary conditions were set to each face once the model was created, as seen in Figures 3 and 4.

### Governing Equations

In Reynolds averaging, the variable in the Navier–Stokes equations in notation given below are decomposed into mean and fluctuation components similar to velocity decomposition [11]

$$u_i = \bar{u}_i + u_i' \quad (1)$$

Where  $u_i$  is the instantaneous fluid velocity,  $u_i'$  is the velocity fluctuation, and  $\bar{u}_i$  is the time-averaged value of  $u_i$  at a point.

Table 1. Variables of the work

Variable	Values
Blocking Ratio (BR)	0.1-0.2-0.3
VGs Number	1-2-3
Attack angle ( $\theta$ )	0-30-45
Aspect Ratio (AR)	1-1.5-2

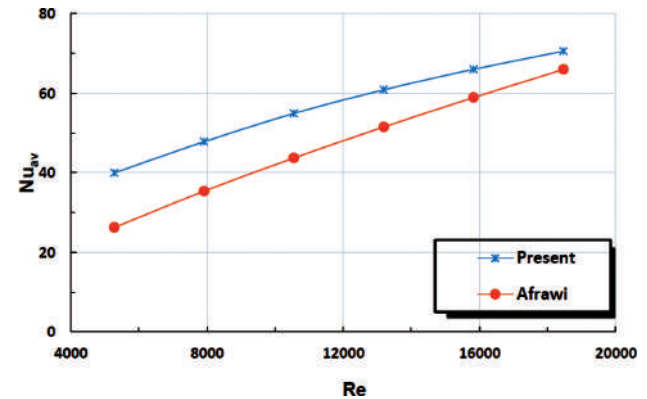


Figure 6. comparison of the present CFD prediction with experimental data from Afrawi [12].

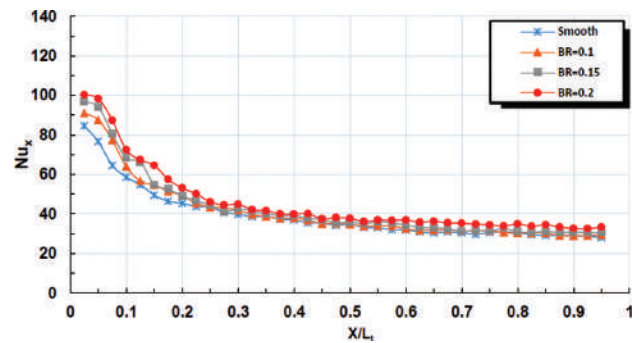


Figure 7. Variation of local Nusselt number with blocking ratio (BR).

To solve the problem, the following assumption are made

- Steady state flow
- The properties are constant
- Radiation is neglected

### Conservation of mass

Continuity equation characterises the law of conservation of mass which states that the mass of a steady state system will remain constant over time

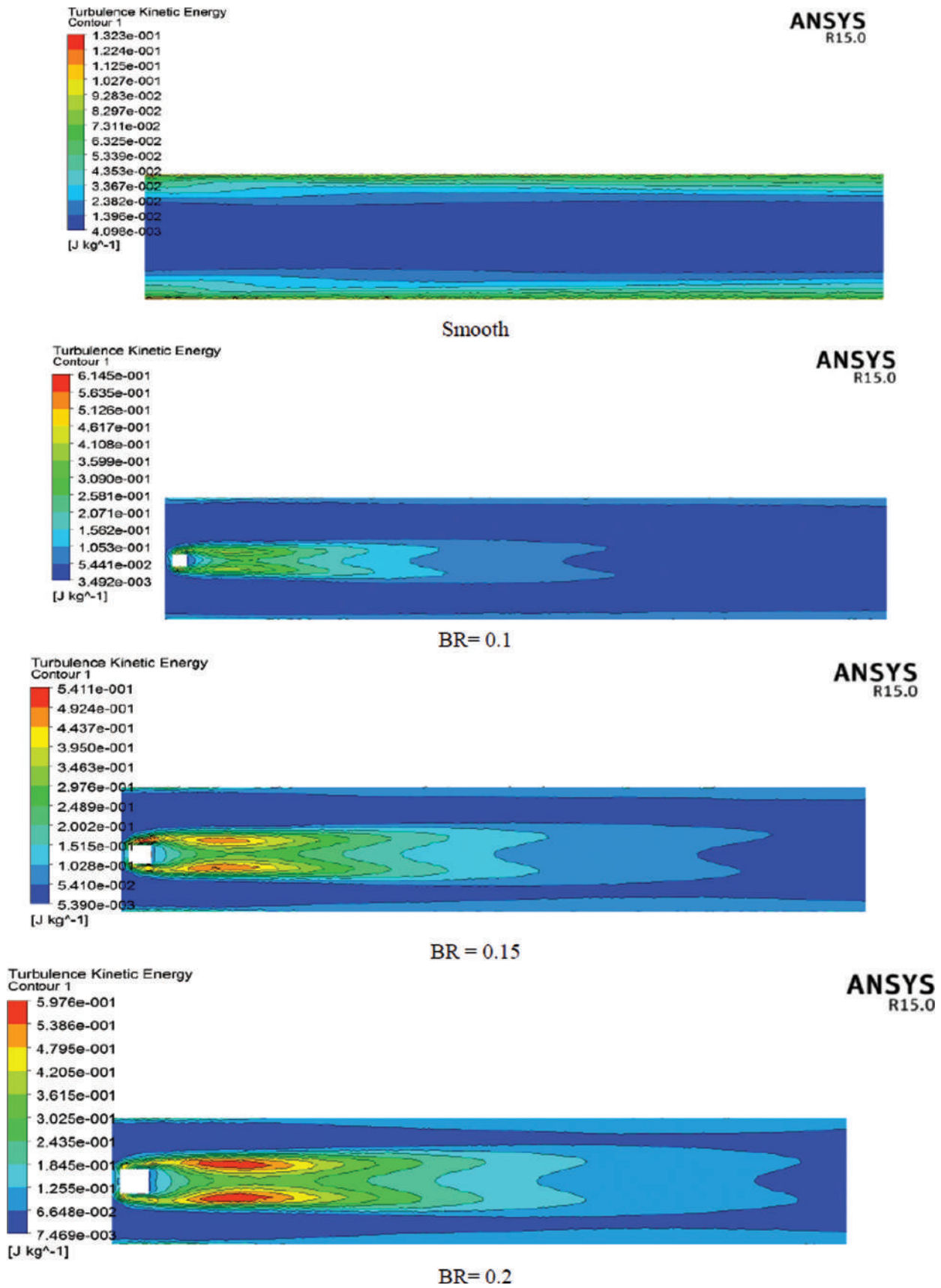


Figure 8. The contours of turbulence kinetic energy for different blocking ratio (BR).

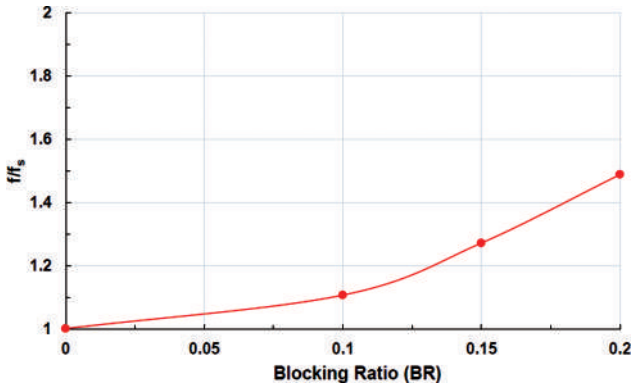


Figure 9. Variation of friction factor with blocking ratio.

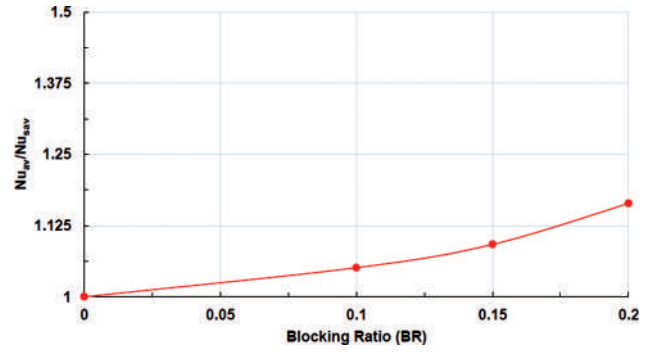


Figure 10. The variation of enhancement of average Nusselt number with blocking ratio.

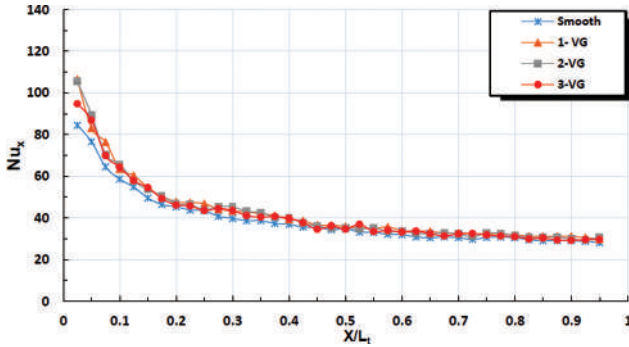


Figure 11. The variation of local Nusselt number with VGs number.

$$\frac{\partial \rho u}{\partial x} + \frac{\partial \rho v}{\partial y} + \frac{\partial \rho w}{\partial z} = 0 \quad (2)$$

as the mass density of fluid is constant the above equation can be written as:

$$\frac{\partial u}{\partial x} + \frac{\partial v}{\partial y} + \frac{\partial w}{\partial z} = 0 \quad (3)$$

Then, the continuity equation is stated as:

$$\frac{\partial u_i}{\partial x_i} = 0 \quad (4)$$

### Conservation of momentum

The principle of conservation of momentum states that: if objects collide in the isolated system, the total momentum before and after collision is the same. In other words, the lost and gained momentum is the same. The momentum equation is stated as [11]

$$\rho \frac{\partial u_i u_j}{\partial x_i} = -\frac{\partial P}{\partial x_i} + \mu \frac{\partial}{\partial x_j} \left( \frac{\partial u_i}{\partial x_j} + \frac{\partial u_j}{\partial x_i} \right) + \rho \frac{\partial}{\partial x_i} \left( -\overline{u'_i u'_j} \right) \quad (5)$$

### Conservation of energy

The law of energy conservation states that the total amount of energy in isolated system remains constant over time [11]. The energy equation can be written as.

$$\rho c_p \frac{\partial u_i T}{\partial x_i} = \frac{\partial}{\partial x_i} \left( \lambda \frac{\partial T}{\partial x_i} - \rho \overline{u'_i T'} \right) \quad (6)$$

Where  $\lambda$ : is thermal conductivity

A number of models is available to simulate the different fluid flows in Fluent. K- $\epsilon$  realizable model is implemented in the present simulation. This model is recommended [14] for the flows with vortices and rotation such as flow inside duct with VGs.

These Partial differential equations are solved with following boundary conditions as shown in figure 5.

- Left face: velocity inlet  $u = \text{velocity}$ ,  $v = w = 0$
- Upper and lower face of test section: heat flux  $q''$
- Right face: pressure outlet  $P = \text{atmospheric pressure}$ .

## RESULTS AND DISCUSSIONS

The heat transfer inside a square duct in the presence of rectangular VGs is investigated numerically. The numerical simulation is carried out with the CFD commercial software Ansys Fluent 15. This investigation aims to demonstrate the effect of blocking ratio (BR), VGs number, attack angle ( $\theta$ ) and VGs aspect ratio (AR) as in table 1. The local convective heat transfer coefficients are estimated on

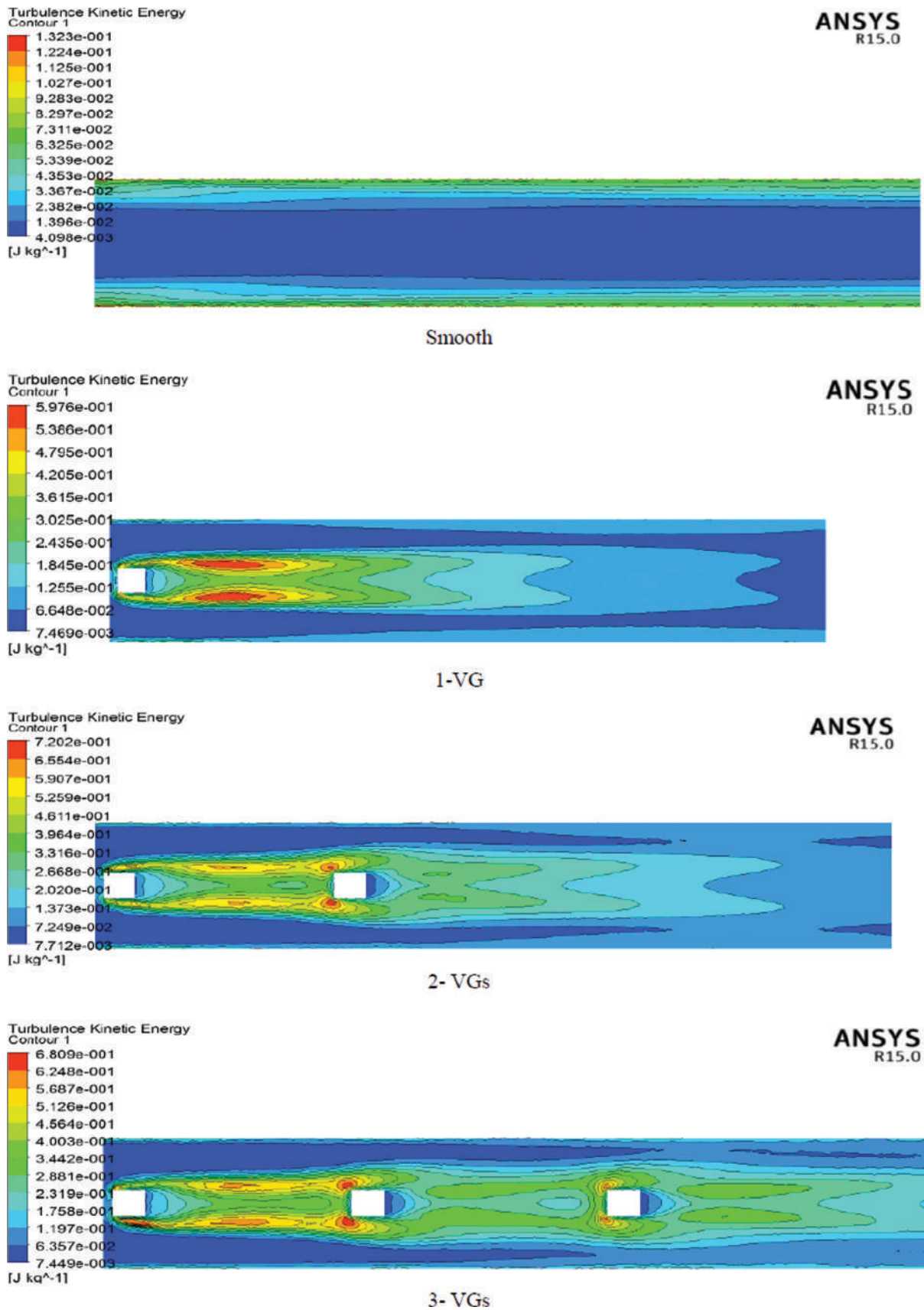


Figure 12. The contours of turbulence kinetic energy (BR = 0.2) for different VGs number.

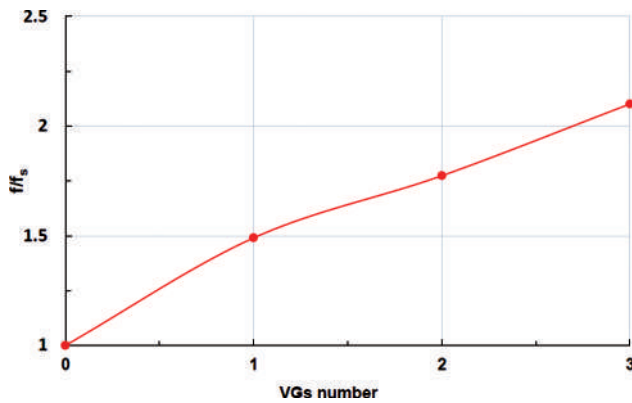


Figure 13. The variation of friction factor with VGs number (BR = 0.2).

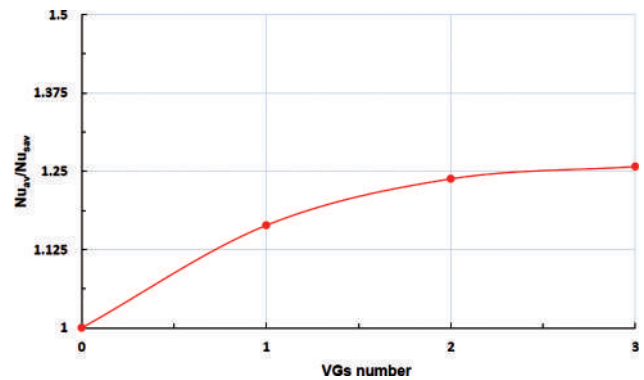


Figure 14. The variation of enhancement of average Nusselt number, (BR = 0.2).

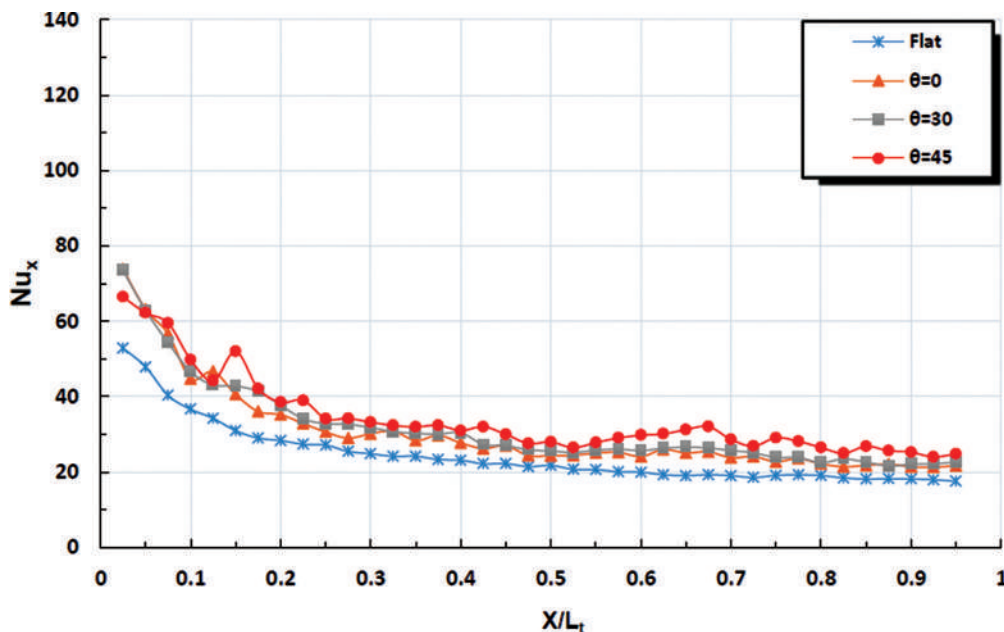


Figure 15. The variation of local Nusselt number with attack angle ( $V = 2$  m/s, BR = 0.2, VGs = 3).

the upper face of the test section. Average Nusselt number is then estimated from average heat transfer coefficient. The distance ( $X$ ) represents the length from the inlet of the test section. Figure 6 depicts a comparison of the obtained data with experimental data from Afrawi [15]. Afrawi correlated the heat transfer inside a smooth duct for turbulent flow conditions. The comparison reveals that the discrepancy at low Reynolds number ( $Re = 5000$ ) is 35% and decreases to reach 6% at  $Re = 18000$ . It is concluded that the present model is reliable to be used for further predictions.

#### Effect of Blocking Ratio (BR)

Figure 7 presents the variation of the local heat transfer rate with the blocking ratio of a VG fixed at the entrance of

the test section. It can be observed that the heat transfer in the region near to the entrance of the test section increases as the blocking ratio increases. This is due to the turbulence generated by VG and which increases with increase of blocking ratio as shown in Figure 8. It can be observed that the blocking ratio has a clear influence on friction factor as shown in Figure 9. The friction factor is about 1.5 times of that of smooth duct when the BR is 0.2. The increase in friction factor can be explained by the increase of fluid retardation as the blocking ratio increases. Figure 10 shows the enhancement ratio of average Nusselt number due to the presence of a VG at the entrance of the test section. The maximum recorded enhancement could reach 17% at BR = 0.2.

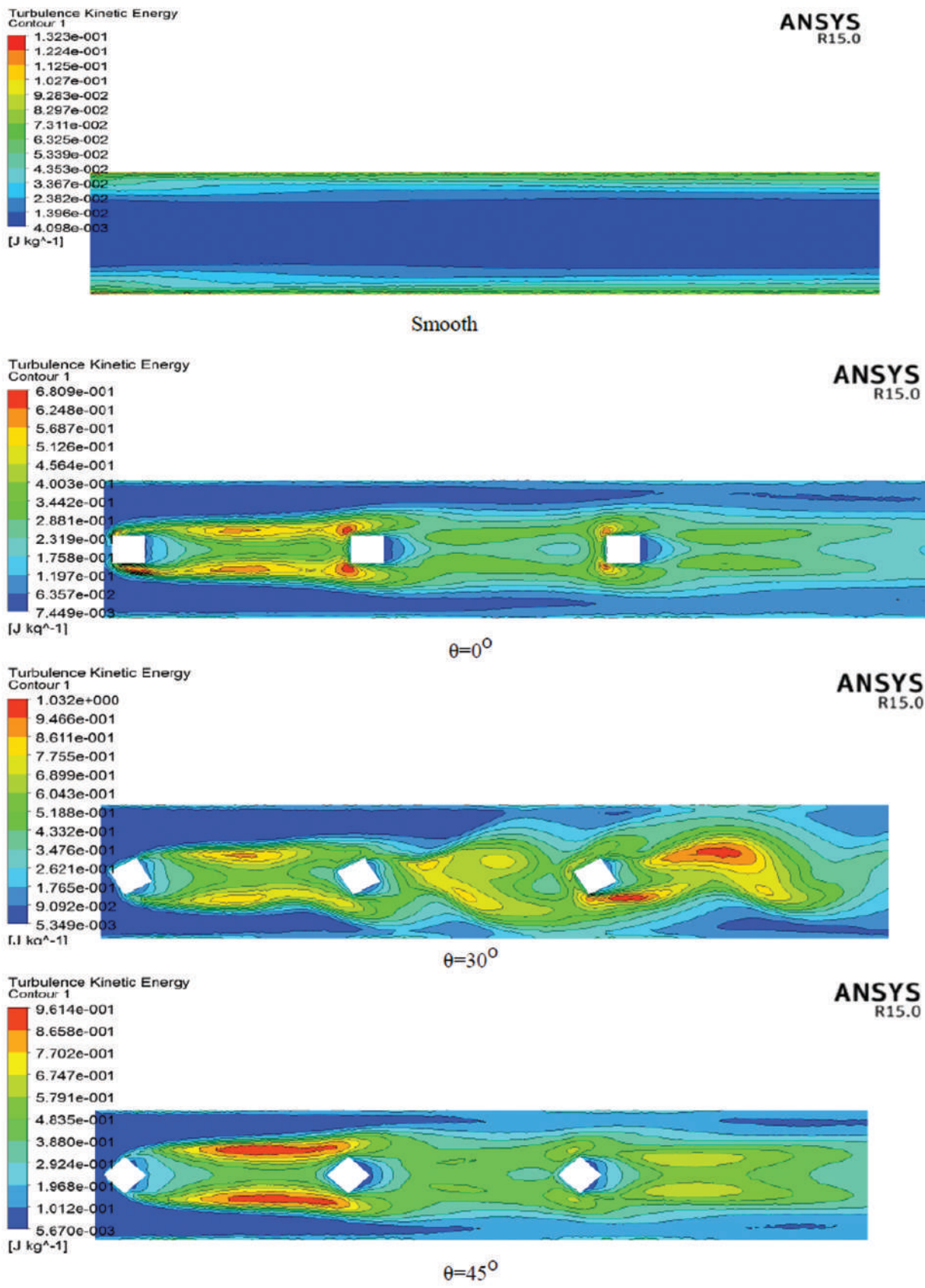


Figure 16. The contours of turbulence kinetic energy (BR=0.2, VGs=3).

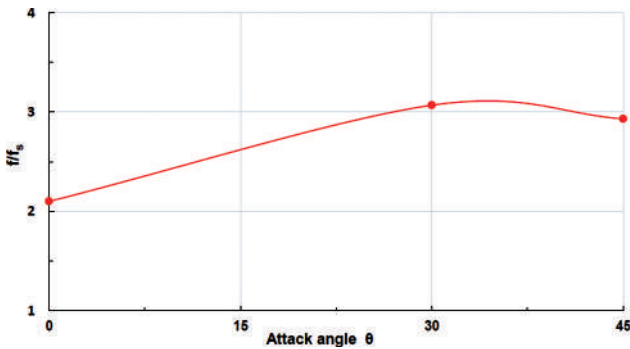


Figure 17. Variation of friction factor with attack angle (BR = 0.2, VGs = 3).

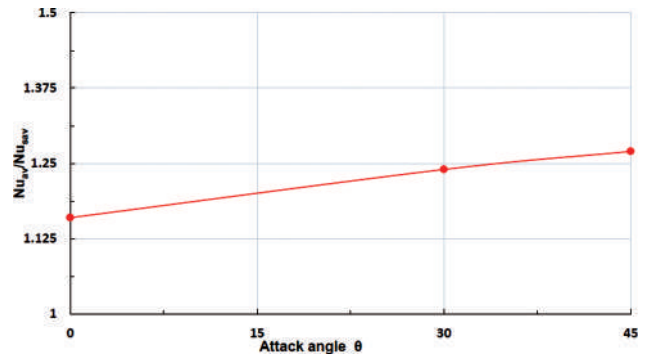


Figure 18. The variation of enhancement of average Nusselt number with attack angle (BR = 0.2, VGs = 3).

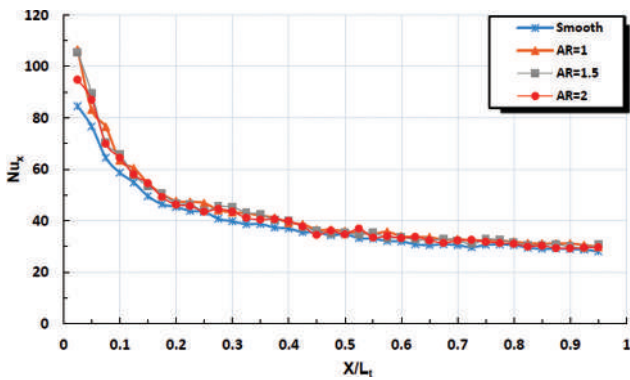


Figure 19. The effect of aspect ratio on local Nusselt number (BR=0.1, VGs=2).

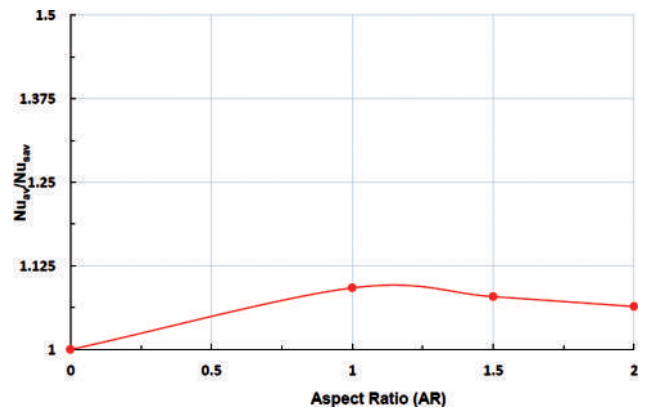


Figure 20. The enhancement of average Nusselt number by aspect ratio (BR=0.1, VGs=2).

**Effect of VGs Number**

The variation of the local heat transfer and VGs number is depicted in Figure 11. The results reveal an enhancement of heat transfer with the increase of VGs number until certain bounds. This enhancement is due to increased turbulence level. The increase in turbulence level can be seen clearly in Figure 12. Also the VGs number has a significant effect on the friction factor. As VGs number increases, more fluid is obstructed which leads to higher pressure drop and higher friction factor as depicted in Figure 13. The enhancement of average Nusselt number for different VGs number compared to smooth duct is shown in Figure 14. The enhancement reaches 27% for 3 VGs and BR = 0.2. The comparison between the graphs of heat transfer and the friction factor shows that the heat transfer increased by 10% while the friction increased by 30% by adding the third VGs. This is an indication that the optimum number of the VGs is 2.

**Effect of Attack Angle ( $\theta$ )**

The effect of the VGs attack angle on the local heat transfer is depicted in figure 15 for case of blocking ratio

(BR = 0.2), velocity ( $V = 2\text{m/s}$ ) and VGs number ( $VGs = 3$ ). In the region between  $X/L_t = 0.025$  and  $X/L_t = 0.2$ , the effect of the attack angle on heat transfer is not clear. This significant effect of effect can be observed for  $X/L_t > 0.2$ . The attack angle has a remarkable effect on of the turbulence of the flow as can be seen in Figure 16. The effect of attack angle on the friction factor is shown in Figure 17. The friction factor increases with the increase on attack angle until =  $35^\circ$ . Then, due to the change of flow around the VG from flow on flat surface to more streamlined surface with changing the angle. The enhancement of average Nusselt number due to the effect of attack angle is given in Figure18 which shows increase by 27%.

**Effect of Aspect Ratio (AR = length/width)**

The effect of aspect ratio on local heat transfer can be seen in Figure19 for VGs = 2 and blocking ratio, BR = 0.1. The local heat transfer is not strongly affected with the change of aspect ratio. From Figure 20, it can be observed that average Nusselt number is affected adversely with aspect ratio. This result can be explained by the change in turbulence level given in Figure 21 which shows the

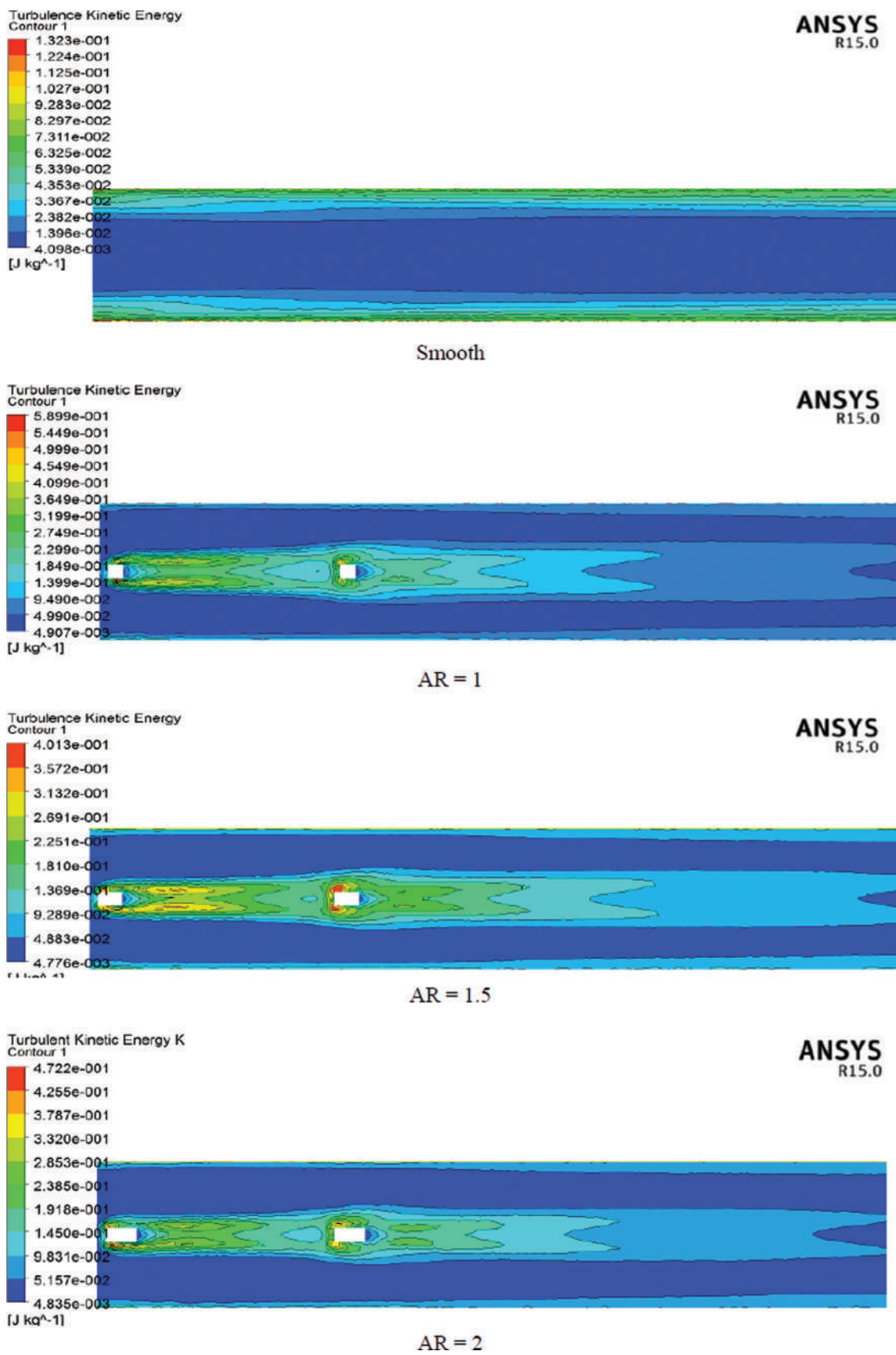
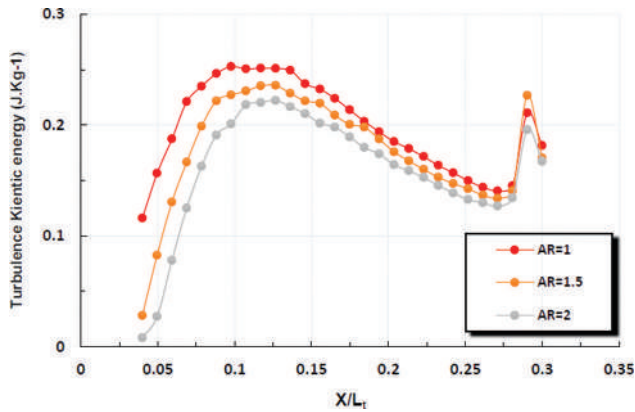
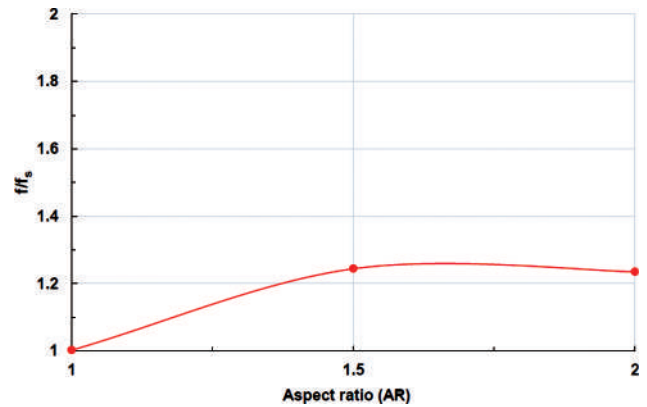


Figure 21. The contours of turbulence kinetic energy for different aspect ratio (BR=0.1, 2-VGs)



**Figure 22.** The variation of turbulence kinetic energy with Aspect ratio (BR = 0.1 , VGs=2).



**Figure 23.** The effect of VGs aspect ratio on the friction factor (BR = 0.1, VGs = 2).

contours of turbulence kinetic energy which decreases as aspect ratio increases. Due to the increase of the weak region effect with larger aspect ratio, the mixed flow region goes further down from the VGs which leads to decreasing in heat transfer as shown in Figure 22. This result supported by the finding from SedatDogru [16]. The aspect ratio (AR) has no significant effect on pressure as shown in Figure 23.

## CONCLUSIONS

This paper numerically investigates the thermal hydraulic performance of a heated square duct with the influence of rectangular VGs (Vortex generators) fitted on the duct-centre line. The Reynolds number was fixed at 5000. The tested parameters are the blocking ratio, BR = 0.1, 0.15, 0.2; VGs number = 1, 2, 3; attack angle,  $\theta = 0, 30, 45^\circ$ ; and aspect ratio, AR = 1-1.5-2. The main conclusions can be summarized as follows :

1. In general, the VGs have a positive influence on heat transfer due to the augmentation in turbulence level. The maximum enhancement in average heat transfer could reach 25 %.
2. The heat transfer increases with the increase in blocking ratio. The heat transfer enhancement for one rib and BR=0.2 is 17%.
3. The number of VGs has a strong effect on heat transfer. The enhancement ranges from 17% for one VG to 28 for 3 VGs for BR = 0.2.
4. The VGs at angle  $45^\circ$  produce the highest heat transfer enhancement due to the strong mixing.
5. The heat transfer seems to decrease with the increase of aspect ratio.
6. The pressure drop of all cases increased faster than heat transfer . this need to be considered when using the vortex generators in any thermal system.

## NOMENCLATURE

AR	aspect ratio
BR	blocking ratio
Cp	Specific heat at constant pressure (kJ/kg.K)
$D_h$	Hydraulic diameter of the duct (m)
f	friction factor
$f_s$	friction factor for smooth duct
Le	Entrance region length (m)
$L_{ex}$	Exhaust region length (m)
$L_t$	Test section length (m)
$Nu_{av}$	Average Nusselt number
$Nu_{sav}$	Average Nusselt number for smooth duct
$Nu_x$	Local Nusselt number
P	Pressure (Pa)
Re	Reynolds number
T	Temperature (K)
u	x-component of velocity (m/s)
ui	Instantaneous fluid velocity (m/s)
$\bar{u}_i$	Time-averaged value of ui at a point (m/s)
$u'_i$	Velocity fluctuation (m/s)
v	y-component of velocity (m/s)
w	z-component of velocity (m/s)
VGs	Vortex generators
X	Distance from the entrance of the test section (m)
$\theta$	Attack angle ( $^\circ$ )
$\lambda$	Thermal conductivity (W/m.K)
$\mu$	Dynamic viscosity (Pa.s)
$\rho$	Density (kg/m <sup>3</sup> )

## AUTHORSHIP CONTRIBUTIONS

Authors equally contributed to this work.

## DATA AVAILABILITY STATEMENT

The authors confirm that the data that supports the findings of this study are available within the article. Raw data that support the finding of this study are available from the corresponding author, upon reasonable request.

## CONFLICT OF INTEREST

The author declared no potential conflicts of interest with respect to the research, authorship, and/or publication of this article.

## ETHICS

There are no ethical issues with the publication of this manuscript.

## REFERENCES

- [1] Ralph L, Nae H. Principles of enhanced heat transfer. CRC Press; 2005.
- [2] Dipak P, Pati R. Passive heat transfer augmentation methods in a circular tube: A Review Int J Innov Res Sci Eng Technol 2017;6:512-526.
- [3] Gaurav A, Manoj M, Sameer K. Thermo-hydrodynamics of developing flow in a rectangular mini-channel array. 20th National and 9th International ISHMT-ASME Heat and Mass Transfer Conference 2010.
- [4] Shivaji V, Rupa S. Numerical and experimental investigations on performance evaluation of a conical offset vortex generator inserts to improve convective heat transfer coefficient. J Therm Eng 2020;6:858-872. [\[CrossRef\]](#)
- [5] Mohd Z, Sujit N, Dipankar B. Numerical analysis to predict the optimum configuration of fin and tube heat exchanger with rectangular vortex generators for enhanced thermohydraulic performance. Heat and Mass Transfer 2020;56:2159-2169. [\[CrossRef\]](#)
- [6] Hanbar A, Faezeh N, Ali A, Farzad P. Wings shape effect on behavior of hybrid nanofluid inside a channel having vortex generator. Heat and Mass Transfer 2018;55:1696-1983. [\[CrossRef\]](#)
- [7] Dongxu J, Manman Z, Ping W, Shasha X. Numerical investigation of heat transfer and fluid flow in a solar air heater duct with multi Vshaped ribs on the absorber. Energy 2015;89:178-190. [\[CrossRef\]](#)
- [8] ZhiminH, Zhiming X, Jingtao W. Numerical simulation on heat transfer characteristics of rectangular vortex generators with a hole. Int J Heat Mass Transf 2018;126:993-1001. [\[CrossRef\]](#)
- [9] Zhang Q, Wang L. Numerical study of heat transfer enhancement by rectangular winglet vortex generator pair in a channel. Adv Mech Eng 2016;8:1-11. [\[CrossRef\]](#)
- [10] Ongnan X, Shaofei Z, Weihong Z, Bengt S. A numerical study of flow structure and heat transfer in a square channel with ribs combined downstream half-size or same-size ribs. Appl Therm Eng 2013;61:289-300. [\[CrossRef\]](#)
- [11] Nianben Z, Wei L, Zhichun L, Peng L, Feng S. A numerical study on heat transfer enhancement and the flow structure in a heat exchanger tube with discrete double inclined ribs. Appl Therm Eng 2015;90:232-241. [\[CrossRef\]](#)
- [12] Farzad P, Mahdi M, Ghanbarali S, DavoodT, Omid A. The numerical investigation of angle of attack of inclined rectangular rib on the turbulent heat transfer of Water-Al 2O3 nanofluid in a tube. Int J Mech Sci 2017;131:1106-1116. [\[CrossRef\]](#)
- [13] Nil S, Bhagoria J. A numerical investigation of square sectioned transverse rib roughened solar air heater. Int J Therm Sci 2014;79:11-131. [\[CrossRef\]](#)
- [14] ANSYS. ANSYS Fluent Theory Guide 2016:1-814.
- [15] Alfarawi S, Abdel-Moneim S, Bodalal A. Experimental investigations of heat transfer enhancement from rectangular duct roughened by hybrid ribs. Int J Therm Sci 2017;118:123-138. [\[CrossRef\]](#)
- [16] Sedat D, Tural T, Harun Z. Effects of vortex generator aspect ratio on enhancement of heat transfer in a straight channel. 1<sup>st</sup> International Mediterranean Science and Engineering Congress 2016:3378-3386.